Available online at www.CivileJournal.org

Civil Engineering Journal

(E-ISSN: 2476-3055; ISSN: 2676-6957)

Vol. 10, No. 11, November, 2024

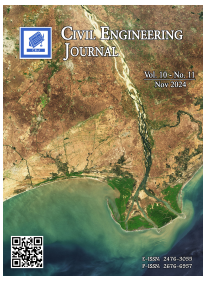

Performance of Asphalt Mixtures Modified with Nano-Eggshell Powder

A. Hadi Zghair Chfat [1], Haryati Yaacob [1*], N. H. Mohd Kamaruddin [2], Z. Hazim Al-Saffar [3], R. Putra Jaya [4]

[1] *Faculty of Civil Engineering, Universiti Teknologi Malaysia, 81310, UTM, Johor Bahru, Malaysia.*

[2] *Faculty of Civil Engineering and Built Environment, Universiti Tun Hussein Onn Malaysia, Johor Bahru 86400, Malaysia.*

[3] *Building and Construction Engineering Department, Engineering Technical College of Mosul, Northern Technical University, Mosul, 41002, Iraq.*

[4] *Faculty of Civil Engineering Technology, Universiti Malaysia Pahang Al-Sultan Abdullah, 26300, Kuantan, Pahang, Malaysia.*

Received 01 May 2024; Revised 22 September 2024; Accepted 06 October 2024; Published 01 November 2024

Abstract

Primary issues in pavement engineering, such as rutting, moisture damage, and fatigue cracking, have prompted numerous studies aimed at improving pavement performance. Utilizing biomaterial waste to modify bitumen through nanotechnology is a promising approach to improve asphalt-mixture properties and aligns with goals of sustainability and reducing the dependence on non-renewable resources. Therefore, the primary objective of this study was to investigate the effect of nano-eggshell powder (NESP) as a sustainable bio-modifier for bitumen on the mechanical properties of asphalt mixtures. To achieve this, asphalt mixtures containing 0% (control), 5%, and 9% NESP were developed, and their mechanical properties were investigated through various tests such as moisture damage, Marshall immersion stability, resilient modulus, dynamic creep, double-punch shear, water immersion, and wheel tracking. The results showed that NESP reduced the moisture susceptibility of the mixtures by increasing their tensile strength ratio. Additionally, the durability of the asphalt mixtures improved as the NESP content was increased. Moreover, the addition of NESP significantly enhanced the resilient modulus and dynamic creep of the asphalt mixtures. The double-punch test revealed that the NESP improved the rutting and fatigue resistance of the asphalt mixtures. Furthermore, the water-immersion test indicated that NESP enhanced the adhesion properties between the bitumen and the aggregate. Finally, the wheel-track test results suggested that the mixtures modified with NESP exhibited a lower rut depth than the control mixtures. Notably, 9% NESP was optimal for enhancing the mechanical properties of the asphalt mixture. The study demonstrated that using NESP as a bio-modifier for bitumen is feasible and offers a more sustainable alternative to traditional bitumen additives.

Keywords: Nano-Eggshell Powder; NESP-Modified Asphalt Mixture; Adhesion; Moisture Damage; Rutting.

1. Introduction

Pavements are essential infrastructure components that serve as the foundation for transportation systems, facilitating the movement of people and goods. However, significant increases in vehicular traffic, axle loads, pedestrians, and fluctuating temperatures contribute to early pavement failure. Bitumen, a naturally occurring hydrocarbon derived from petroleum distillation, is a primary component in asphalt mixtures used to construct pavements. However, petroleum-based resources are non-renewable, and sustainability and carbon neutrality by 2050 have become the primary goals of several countries [1, 2]. Therefore, there is an urgent need to enhance the properties of asphalt mixtures, extend their service life by using modifiers, and search for sustainable alternatives to bitumen [3,4].

Researchers have used various additives and modifiers, such as polymers, and waste materials, such as rubber, ash, and fibers, to enhance the properties of bitumen and the performance of asphalt mixtures [4-10]. However, these

* Corresponding author: haryatiyaacob@utm.my

http://dx.doi.org/10.28991/CEJ-2024-010-11-016

modifiers have several drawbacks, including instability and incompatibility with bitumen owing to the substantial differences between their densities, polarities, and molecular weights [11-14]. Thus, improving the characteristics of these modifiers to meet the desired specifications may incur extra costs, rendering them impractical for large-scale implementation [15, 16].

Recently, the application of nanomaterials to enhance the properties of bitumen and asphalt mixtures has garnered considerable interest. This is attributed to the unique characteristics of nanomaterials, such as large surface areas, high surface free energy, and excellent dispersion within the bitumen matrix [17]. Various nanomaterials, such as nano silica (NS), nano clay (NC), nano titanium dioxide (TiO_2), carbon nanofiber (CNF), and nano zinc oxide (ZnO), have been used to modify bitumen [4, 18]. Bhat et al. [19] reported that nano SiO_2 and nano Al_2O_3 enhance the stability, moisture-damage resistance, and resilient modulus (Mr) of asphalt mixtures. Aljbouri et al. [7] studied the effects of incorporating various nanomaterials, including NS, nano carbonate calcium (NCC), NC, and nano platelet hydroxyapatite (NP), on the durability of asphalt mixtures and found that they significantly enhance their performance. Abdel-Wahed et al. [20] evaluated the performances of asphalt mixtures modified with NS and NC and revealed that these nanomaterials enhance the stability, moisture resistance, and rutting resistance of these mixtures.

However, most nano-modifiers are considered impractical for widespread application in road construction because of their high costs, often resulting in a 60–150% increase in the original bitumen cost [21]. Therefore, their use has been primarily limited to bitumen modification, and few studies have explored the application of nanotechnology to asphalt mixtures [22]. Moreover, certain nanomaterials pose risks to the environment, as well as the health and safety of humans [11, 23], primarily owing to their dispersion in air and the possibility of them leaching into groundwater during pavement construction and asphalt laying. This dispersion can contribute to air and water pollution, leading to various health issues and, in some cases, cancer incidence [24]. Therefore, the fundamental challenge lies in using environment-friendly nanomaterials that can be produced in large quantities at low cost. A potential solution is converting waste materials into nanomaterials to modify asphalt mixtures. This approach can contribute to environmental protection by converting waste into valuable resources and aligns with the principles of sustainable development. Additionally, it offers various benefits to the construction and resource-recovery industries.

Exploring biomaterial waste and investigating their use to modify asphalt mixtures through nanotechnology presents excellent opportunities because of their availability, low costs, and environmental benefits [25-27]. Additionally, as improper disposal of biological waste can have substantial environmental impacts, incorporating them into road construction can help mitigate their hazardous effects [28]. Biological waste materials such as fish shells, oyster shells, crayfish shells, bio-oil, and lignin have been used to modify bitumen and exhibited promising results [29-31].

Eggshell waste has received significant attention owing to its low cost and widespread availability compared with other types of biological waste, and recycling them transforms them into valuable resources [3, 32, 33]. Moreover, it is the 15th leading cause of environmental contamination [34], releasing high levels of pollutants and odours during decomposition because of the presence of compounds such as ammonia and hydrogen sulphide [35-37]. It may also contain bacteria such as Salmonella and Escherichia coli (E. coli), which can cause food poisoning [38]. The disposal of eggshell waste is a significant issue in many countries, primarily because of the high costs associated with landfills and their adverse environmental impacts [39]. Estimates suggest that nearly 7 million tonnes of eggshell waste is generated annually [40], and egg production is expected to reach 90 million tonnes by 2030 [41].

As eggshells contain high concentrations (>96%) of calcium carbonate ($CaCO_3$) [28, 42], numerous studies have investigated the potential application of eggshell waste as a raw material in the chemical, engineering, and environmental fields [43-45]. However, studies on their incorporation into asphalt mixtures as bitumen modifiers for pavement construction are limited. Masri et al. [46] reported that using 4% of eggshell powder to modify bitumen increases the Mr of stone mastic asphalt and found that the cumulative strain of the modified sample was better than that of the unmodified sample. Additionally, Huang et al. [28] investigated the effects of using different proportions (3, 6, 9, and 12%) of eggshell powder as bitumen modifiers on the rutting and moisture-damage resistance of asphalt mixtures. Their results indicated that higher amounts of eggshell powder enhance the rutting and moisture-damage performance.

However, these studies focused on using eggshell powder at the microscale in asphalt mixtures, without addressing the compatibility and stability issues between eggshell powder and bitumen. The substantial disparities between the volume and molecular weights of eggshell powder and bitumen lead to phase separation at high temperatures, which diminishes the benefits of their addition, particularly when used on a large scale [12, 13, 15, 47]. Recently, Zghair Chfat et al. [48] incorporated nano-eggshell powder (NESP) at various concentrations (1, 3, 5, 7, and 9% by weight of bitumen) as a bio-modifier for bitumen and assessed the physical, rheological, and microstructural properties of NESP-modified bitumen. Their findings revealed that NESP demonstrated significant potential for enhancing the compatibility, thermal stability, rutting resistance, and adhesion of bitumen.

A previous study that incorporated NESP into bitumen focused exclusively on evaluating the properties of NESP-modified bitumen [48]. However, it did not address the mechanical properties of asphalt mixtures containing NESP, which is crucial for determining the extent of the benefits derived from this modification. Therefore, this study assessed the effect of NESP on the mechanical properties and performance of asphalt mixtures through several tests, including moisture-damage resistance, Marshall immersion, resilient modulus, dynamic creep, double-punch (DP) shear, water immersion, and wheel-tracking.

2. Material and Methods

2.1. NESP

Eggshell waste was prepared before converting it into a nanosize. This process included cleaning, washing, sterilization, and removal of the shell membranes by boiling in an aqueous NaCl solution for 1 h [28] and then drying in an oven at 100 °C for 24 h. Subsequently, they were ground into a powder and sieved to achieve a granular size of 45 µm. Finally, a planetary ball mill was used to produce NESP samples with particle sizes of <100 nm through trial and error using durations of 2, 4, and 6 h. The entire process is shown in Figure 1. A particle-size analyzer (PSA) was used to assess the particle size, and energy-dispersive X-ray (EDX) microanalysis was conducted to investigate the chemical composition of NESP. The instrument model BETA204A was used to measure the specific surface area, and a micromeritics instrument was employed to determine the specific gravity of the NESP samples. PSA revealed that the optimal nanosize was 73.8 nm, which was achieved after 6 h of milling, as shown in Figure 2. EDX analysis of the NESP sample revealed high O, Ca, and C contents, as shown in Figure 3, which are consistent with the presence of $CaCO_3$ in the NESP. Additionally, the surface area and specific gravity of the particles were 57.621 m²/g and 2.7, respectively. The physical properties and chemical composition of the NESP sample are listed in Table 1.

Figure 1. Preparation of nano-eggshell powder

Table 1. Properties of NESP obtained through 6 h of milling

	Properties	Value
Physical properties	Average size (nm)	73.8
	Specific surface area (m^2/g)	57.621
	Specific gravity	2.7
Chemical composition	Elemental analysis (%)	C = 11.4
		O = 48.9
		Ca = 39.2
		Mg = 0.3
		Si = 0.2

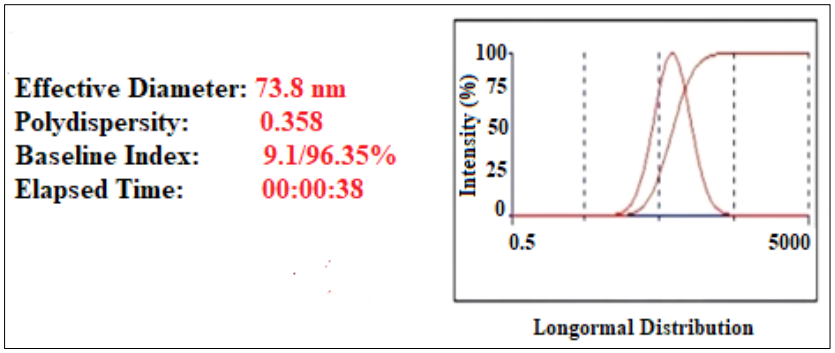

Figure 2. PSA results of NESP obtained through 6 h of milling

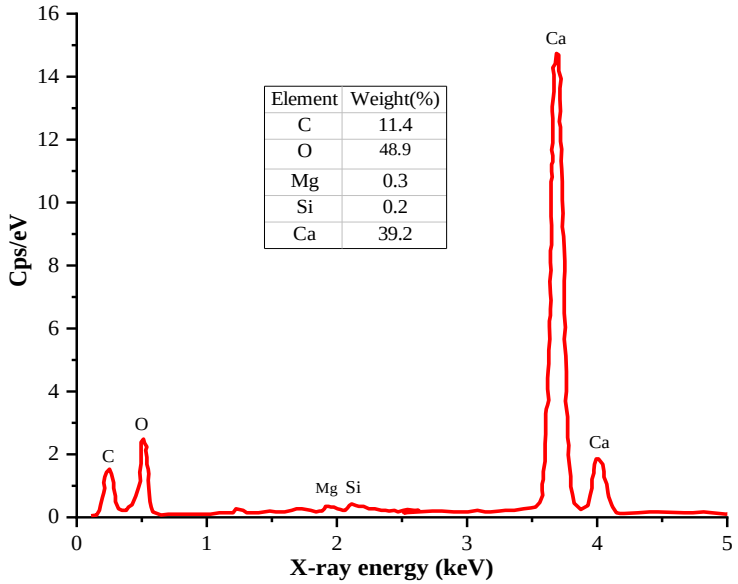

Figure 3. EDX spectra of NESP obtained through 6 h of milling

2.2. Bitumen

Bitumen PEN 60/70 was sourced from the Kemaman Bitumen Company, Malaysia, and thoroughly evaluated before it was incorporated into the asphalt mixture. Table 2 presents the physical and rheological properties of the bitumen used in this study, which met both the local requirements and international specifications.

Table 2. Properties of bitumen PEN 60/70

Description	Result	Requirement [49]	Specification
Penetration at 25 ℃ (dmm)	62.0	60–70	ASTM D5/D5M [50]
Softening point (℃)	49.2	49–56	ASTM D36/D36M [51]
Viscosity at 135 ℃ (Pa·s)	0.606	<3 Pa.s	ASTM D4402/D4402M [52]
Rutting parameter, G*/sinδ (kPa) at 64 ℃	2.65	>1 kPa	ASTM D7175 [53]

2.3. Aggregate

A granite aggregate with a nominal maximum size of 14 mm (AC14) was used in this study; its physical properties are listed in Table 3. A high specific gravity indicates that the aggregate is durable. Additionally, it featured a water absorption rate of <2%, suggesting that it had a low tendency to absorb bitumen, thereby requiring less bitumen. Additionally, its aggregate impact value (AIV), aggregate crushing value (ACV), flakiness index, and elongation index satisfied these requirements [48], indicating that it is suitable for road construction and highly durable. Figure 4 shows the particle-size distribution of the aggregate. Based on this distribution, the median gradation was determined to fall within the lower and upper limits specified by the Malaysian Public Works Department—Jabatan Kerja Raya (JKR [49]).

Table 3. Physical properties of the granite aggregate

Test	Value	Requirement [49]	Specification
Specific gravity	2.65 (Coarse)	-	ASTM C127 [54]
	2.56 (Fine)	-	ASTM C128 [55]
Water absorption (%)	0.651(Coarse)	<2	ASTM C127 [54]
	1.21 (Fine)	<2	ASTM C128 [55]
Aggregate impact value (AIV) (%)	24.7	<30	BS EN 1097-2 [56]
Aggregate crushing value (ACV) (%)	17	<30	BS EN 1097-2 [56]
Flakiness Index (%)	10	<25	BS EN 933-3 [57]
Elongation Index (%)	14	<25	BS EN 933-4 [58]

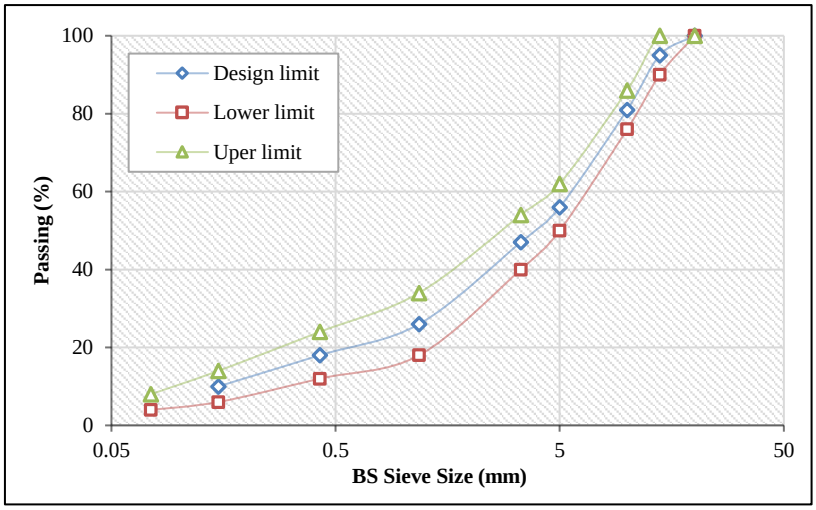

Figure 4. AC14 gradation

2.4. Preparation of Modified Bitumen

NESP-modified bitumen was prepared by incorporating 0, 5, and 9% of NESP into bitumen using a high-shear mixer, as illustrated in Figure 5. These proportions were selected to assess the sensitivity of the NESP content in bitumen based on previous studies that have incorporated nanomaterials into bitumen [59-62]. The mixture was blended at a speed of 3000 rpm for 40 min at a temperature of 160 °C. The mixing parameters were selected based on those reported in previous studies that incorporated nanomaterials into bitumen. The selected mixing speed prevented the potential agglomeration of the NESP, which primarily occurs at speeds lower than 3000 rpm [4]. Moreover, the selected temperature ensured sufficient fluidity and prevented bitumen aging at higher temperatures [48], whereas the selected blending time ensured the complete dispersion of NESP in bitumen [48].

Figure 5. Bitumen modification through high-shear mixing

3. Experimental

3.1. Optimal Bitumen Content (OBC)

In this study, the OBC was calculated based on the Marshall method in accordance with ASTM D 6927 [63]. The specimens were compacted by employing 75 blows on each side of cylindrical samples with a diameter of 101.6 mm and thickness of 63.5 cm. The mixing and compaction temperatures were determined for mixtures with viscosities of 0.170 ± 0.02 and 0.280 ± 0.03 Pa.s, respectively [64]. Additionally, the OBC of the unmodified mixtures was determined to be 5.2% and verified with the JKR specifications [49], as listed in Table 4. This ratio was implemented for both the unmodified and NESP-modified asphalt mixtures to ensure that the amount of bitumen did not confound the test-data analysis [19, 59, 64-66].

Table 4. Marshall stability and properties of the unmodified mixtures

Parameter	Test Value	Specification [49]
Stability (N)	22412.7	>8000
Flow (mm)	3.22	2.0–4.0
Stiffness (N/mm)	6960.5	>2000
Voids In Mix (VIM) (%)	3.74	3–5
Voids Filled with Bitumen (VFB) (%)	71.5	70–80
OBC (%)	5.20	4–6

3.2. Asphalt-Mixture Performance Tests

The performance of the asphalt mixture was evaluated through various tests, including moisture-damage resistance, Marshall immersion stability, modulus of resilience, dynamic creep, DP shear, water immersion, and wheel tracking, and the results were rigorously analyzed and compared with those of conventional asphalt mixtures. Additionally, because NESP contains a high concentration of $CaCO_3$, its effect on the properties of asphalt mixtures was evaluated by comparing it with those elucidated in previous studies that used pure nano $CaCO_3$ to modify asphalt mixtures. The optimal NESP proportion was determined based on the asphalt mixture performance.

3.2.1. Moisture Susceptibility

The effect of moisture damage on the asphalt mixture was examined through the ASTM D4867/D4867M [67]. Six samples of each mixture type were prepared with 7% ± 0.5% air voids and divided into two groups. The first group was saturated (55–80%) in distilled water for 5 min at 25 °C under 70 kPa in a vacuum vessel. Subsequently, they were submerged in a water bath for 24 h at 60 °C. Thereafter, both groups were maintained at 25 °C for at least 2 h, with the wet group remaining in the water bath and the dry group placed in a plastic bag and soaked in the water bath. An indirect tensile-strength test was conducted on the dry and conditioned samples by applying a loading rate of 50.8 mm/min until failure, as shown in Figure 6. The peak load at failure was used to compute the indirect tensile strength of the conditioned and unconditioned samples using Equation 1. Subsequently, the tensile-strength ratio (TSR) was obtained to evaluate the sensitivities of the asphalt mixtures to moisture using Equation 2.

$$\mathrm{ITS} = \frac{2000\mathrm{P}}{\pi \mathrm{tD}} \quad (1)$$

$$\mathrm{TSR}\ (\%) = \frac{\mathrm{ITS_{cond}}}{\mathrm{ITS_{dry}}} \times 100 \quad (2)$$

where ITS denotes the indirect tensile strength (kPa), P is the maximum load (N), t is the specimen height (mm), D is the specimen diameter (mm), and ITS_{cond} and ITS_{dry} are the average tensile strengths (kPa) of the wet and dry samples, respectively.

Figure 6. Setup of the sample in the ITS apparatus for the indirect tensile-strength test

3.2.2. Marshall Immersion

The Marshall immersion test is a continuation of the Marshall test performed in accordance with the ASTM D1075-07 [68] and is used to assess the moisture sensitivity and durability of asphalt mixtures. In this test, the ability of the mixture to withstand the effects of water and temperature was assessed by exposing it to hot water at 60°C for 30 min, 24 h, and 48 h. Nine samples were divided into three groups of three each. The first group, designated as unconditioned samples, was immersed in a water bath at 60 ± 1 °C for 30 min. The second and third groups were immersed in a water bath at 60 ± 1 °C for 24 and 48 h, respectively, and designated as conditioned samples. Subsequently, all groups were tested at a constant compression rate of 50 ± 5 mm/min until failure, as illustrated in Figure 7. Durability assessments of asphalt pavements are primarily based on the loss of strength or stability, which is typically expressed as an index. Three indices are used to assess pavement durability: retained strength index (RSI) (Equation 3), first durability index (FDI) (Equation 4), and second durability index (SDI) (Equation 5) [69]. A lower RSI indicated lower pavement durability. By contrast, a higher durability index indicates a greater loss of strength or stability, suggesting a low pavement durability [70].

$$\text{RSI}\ (\%) = \frac{S_i}{S_0} \times 100 \tag{3}$$

where S_i is the stability after immersion at time t_i or that of the conditioned specimen, and S_0 is the stability before immersion or that of the unconditioned specimen.

$$\text{FDI} = \sum_{i=0}^{n-1} \frac{S_i - S_{i+1}}{t_{i+1} - t_i} \tag{4}$$

$$\text{SDI} = \frac{1}{t_n} \sum_{i=0}^{n-1} A_i = \frac{i}{2t_n} \sum_{i=0}^{n-1} (S_i - S_{i+1}) \times [2t_n - (t_{i+1} - t_i)] \tag{5}$$

where S_i and S_{i+1} are the RSI percentage after immersion times of t_i and t_{i+1}, respectively, t_n is the total immersion duration of immersion, and Ai represents the square of the lost strength for the i^{th} immersion period.

Figure 7. Marshall-immersion test setup

3.2.3. Resilient Modulus (Mr)

The resilient modulus (Mr) indicates the ability of the asphalt pavement to return to its initial state after being subjected to loading. This non-destructive test was conducted in accordance with the ASTM D7369 [71]. A universal testing machine (UTM-5P) was used to conduct the tests, as illustrated in Figure 8. The tests were conducted at 25 and 40 °C to evaluate the resistance of the asphalt mixtures to fatigue cracking and rutting. Prior to testing, the samples were conditioned for 4 h in the UTM. During the test, they were subjected to a load of 1000 N with a haversine wave pattern. Each sample was subjected to 5 pulses, each involving loading for 0.1 s and resting for 0.9 s. Additionally, each asphalt-mixture sample was tested at various orientations by rotating it 0– 90°. Subsequently, the software calculated its Mr (MPa) as follows:

$$\text{Mr} = \frac{F}{Ht\ (0.27+\mu)} \tag{6}$$

where F is the applied force (N), t is the sample thickness (m), H is the horizontal displacement (m), and μ is Poisson's ratio.

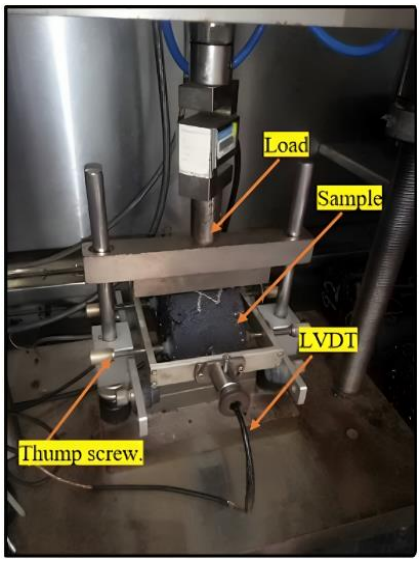

Figure 8. Mr test setup

3.2.4. Dynamic Creep

A dynamic creep test was conducted according to the BS EN 12697-25 [72], which is a destructive test used to assess permanent deformation or rutting. It was conducted using the UTM-5P, and the samples were conditioned at 40°C for 4 h prior to the testing. After conditioning, they were placed inside the machine, with the variable differential transformer positioned on the right- and left-hand sides, as shown in Figure 9. In the first stage, a preload of 150 kPa was applied for 30 s to ensure contact between the load bar and sample. Subsequently, a cyclic-loading stress of 300 kPa was applied for 3600 cycles. The creep-stiffness modulus (CSM; MPa) and creep strain slope (CSS) were then calculated based on the data obtained from the repeated-load creep test as follows:

$$\text{CSM} = \frac{\sigma}{\varepsilon} \tag{7}$$

$$\text{CSS} = \frac{\log \varepsilon_{3600} - \log \varepsilon_{1200}}{\log 3600 - \log 1200} \tag{8}$$

where σ is the applied stress (kPa), ε is the cumulative axial strain at the 3600th cycle (mm), ε3600 is the strain at the 3600th cycle, and ε1200 is the strain at the 1200th cycle.

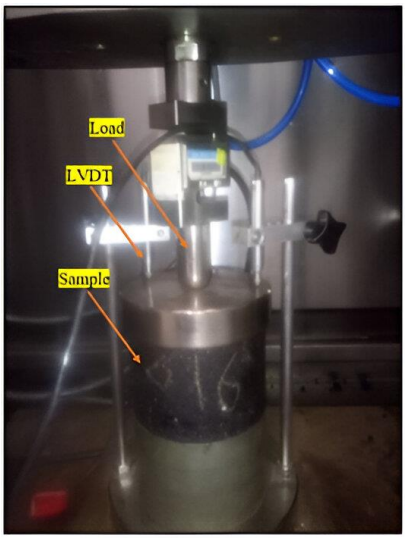

Figure 9. Sample set up inside the UTM-5P machine for the dynamic creep test

3.2.5. DP Shear

The DP shear test, conducted by Jimenez at the University of Arizona [73, 74], was employed to investigate the stripping of the asphalt mixtures. This test, which has been employed in several studies [11, 73-75], was employed not only for the stripping evaluation but also for assessing the rutting and fatigue behavior [11]. Three cylindrical samples

of each mixture type were prepared, with dimensions matching those of the Marshall samples. The first set was immersed in a water bath at 60℃ for 30 min to evaluate rutting, whereas the remaining specimens were tested at 25℃ to assess the fatigue behavior of the asphalt mixture. As illustrated in Figure 10, the sample was positioned between two steel rods (each with a diameter of 25 mm) and tested at a speed of 25.4 mm/min. The DP shear strength was calculated as follows:

$$\sigma t = \frac{P}{\pi(1.2bh - a^2)} \quad (9)$$

where σt is punching stress (Pa), a is the punch radius (mm), h is the specimen height (mm), b is specimen radius (mm), and P is the maximum load (N).

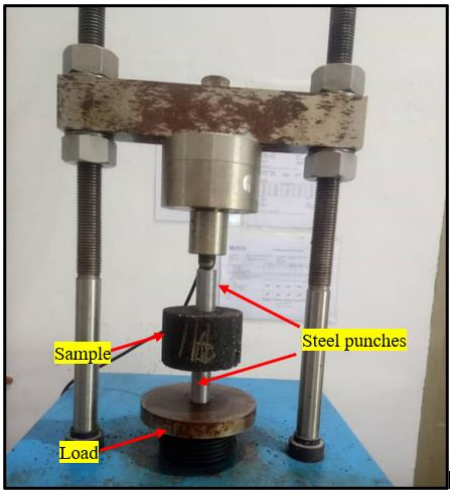

Figure 10. DP test setup

3.2.6. Water Immersion

This test was conducted in accordance with the AASHTO T182 [76] to evaluate the moisture sensitivity of the loose asphalt-coated aggregates. First, a 100-g asphalt-coated aggregate sample was immersed in a 500-ml glass container containing distilled water for 16–18 h at 25℃, as illustrated in Figure 11. Thereafter, the samples were visually examined to determine the proportion of coated material remaining above or below 95%. If the mixture failed to meet the test requirements (less than 95% remaining), it was considered a failure and was avoided owing to its susceptibility to stripping [77].

Figure 11. Water-immersion test setup

3.2.7. Wheel Tracking

Rutting tests were conducted according to the procedure outlined in the AASHTO TP 63-03 [78]. The Asphalt Pavement Analyzer Jr. (APA Jr.; HM-457; Gilson Company Inc., Lewis Center, OH, USA), equipped with an automatic measuring system, was used to evaluate the rut depths of the asphalt mixtures, as depicted in Figure 12. The test involved recording the loading-cycle curves and final rut depth after 8,000 cycles (16,000 passes) under dry conditions at 60℃. Approximately 135 min were required to complete the rutting cycle. These tests were performed on cylindrical samples with a diameter of 150 mm, a height of 75 mm, and an air void content of 7 ± 0.5%. Four specimens were used to represent each set of samples in the test.

Asphalt mixtures may undergo significant deformation during the initial testing phase compared with the final stage. Therefore, determining the rutting rate (RR) (mm/min) is crucial for understanding the overall behaviour of the mixture during the test, and it is calculated as follows [79, 80]:

$$RR = \frac{d_2 - d_1}{15} \quad (10)$$

where d_1 and d_2 denote the rut depths at 45 and 60 min, respectively.

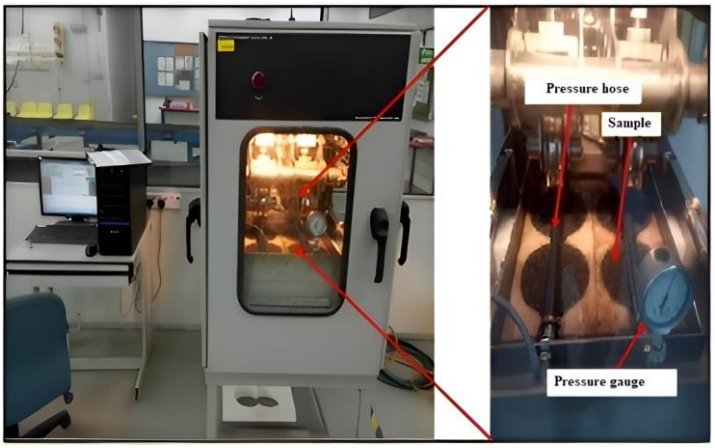

Figure 12. Double-wheel-tracking machine (APA Jr.)

4. Results and Discussions

4.1. Moisture Damage

The susceptibility of asphalt pavements to moisture damage is a significant issue because it deteriorates the adhesion between the aggregate and bitumen, ultimately impacting the performance of the asphalt mixture. In this study, the moisture susceptibilities of both the unconditioned and conditioned samples were evaluated based on the TSR by measuring their ITSs, which are illustrated in Figure 13. Evidently, the ITS values of the wet mixtures are significantly lower than those of dry mixtures. This reduction was anticipated because the presence of water weakened the adhesion between the aggregates and bitumen, thereby decreasing the strength of the asphalt-mixture samples under loading. By contrast, the unconditioned specimens of the NESP-modified asphalt mixtures exhibit significantly higher ITS values, with 9% NESP shown the highest ITS of 1278 kPa, followed by the 5% NESP (1135 kPa), whereas the control mixture exhibits the lowest value (1041 kPa). The higher ITS values can be attributed to the enhanced adhesion between the bitumen and aggregates in the modified mixture than those in the unmodified mixture. This enhancement makes it more difficult to break the bitumen–aggregate bonds. Additionally, bitumen stiffness is an important factor. The incorporation of NESP into bitumen enhances the stiffness and strength of the resulting mixture, thereby increasing its resistance to adhesion failure.

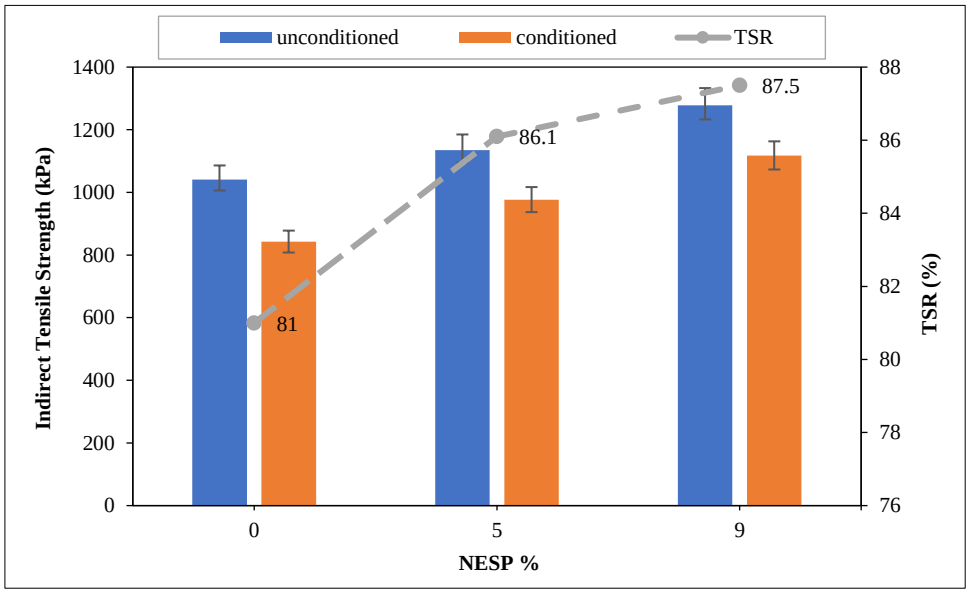

Figure 13. ITS and TSR results of unconditioned and conditioned asphalt-mixture samples

Similarly, after conditioning, the ITS values of the conditioned samples increased as the NESP content was increased, as illustrated in Figure 13. The control mixture exhibited the lowest ITS of 843.0 kPa, whereas the modified mixtures

containing 5% and 9% of NESP registered ITS values of 977.0 and 1118 kPa, respectively. These results indicate that NESP considerably enhances the bitumen–aggregate adhesion under wet conditions. Previous studies reported similar findings, demonstrating that the addition of nano-$CaCO_3$ improved the ITS of asphalt mixtures by enhancing the bitumen–aggregate adhesion [7, 8, 59].

Furthermore, the TSR results illustrated in Figure 13 indicate that all mixtures met the minimum TSR requirement of 80% set by the ASTM D4867/D4867M [67]. Furthermore, the TSRs of the NESP-modified asphalt mixtures were higher than those of the unmodified ones. The phenomenon of moisture failure in asphalt mixtures is attributed to the loss of cohesion within the bitumen or at the bitumen–aggregate interface. Cohesive failure may occur because water molecules are easily attracted to asphaltene molecules, which have stronger polarity than other bitumen components, consequently increasing the distance between these components [81]. As the duration of bitumen conditioning with moisture increases, the failure point shifts from within the bitumen to the bitumen–aggregate interface, leading to a loss of adhesion between the two, and this phenomenon is accelerated at higher temperatures [81]. Therefore, the addition of NESP with a high nonpolar content and superior thermal properties can increase the structural bitumen ratio and enhance its stiffness, thereby mitigating the effects of water and heat [82]. Additionally, owing to its high $CaCO_3$ content, NESP enhances the coating properties of the aggregates by forming molecular layers on their surfaces, thereby increasing the moisture resistance and strength of the samples. According to Hamedi et al. [83], $CaCO_3$ significantly alters the hydrophobic properties of the asphalt mixtures. As the percentage of $CaCO_3$ increases, the aggregates become more hydrophobic, which improves their moisture resistance. Manfro et al. [59] and Aljbouri et al. [7] reported similar results, wherein the susceptibility of asphalt mixtures to moisture decreased with the addition of nano $CaCO_3$.

4.2. Marshall Immersion

The Marshall-immersion test was used to assess the durability of the asphalt mixtures. Figure 14 shows the stability results for various immersion times. The unconditioned samples, which were immersed for 30 min, exhibited higher stabilities as the NESP content increased, with the control, 5% NESP-modified, and 9% NESP-modified asphalt mixtures demonstrating values of 21.59, 22.52, and 27.89 kN, respectively. However, as shown in Figure 14, the stability decreased as the immersion times increased, possibly owing to the deterioration of the adhesion between the aggregates and bitumen caused by heat and water exposure. After immersion for 24 h, the stability values of the control, 5% NESP-modified, and 9% NESP-modified asphalt mixtures decreased by 10, 9.4, and 9.0%, respectively, compared with the unconditioned samples, whereas after immersion for 48 h, they exhibited reductions of 18.0, 16.3, and 15.7%, respectively.

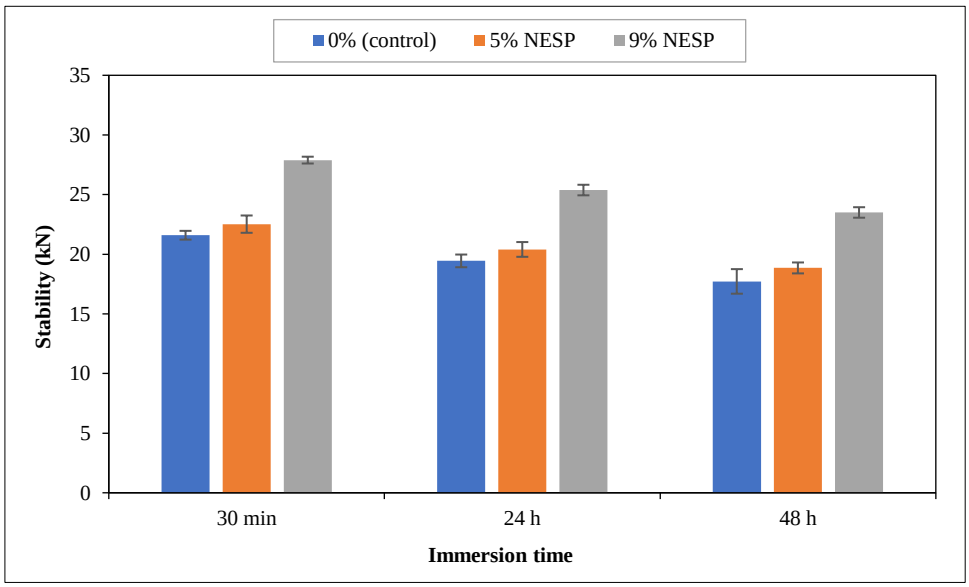

Figure 14. Marshall stability results

The enhancements in the bitumen cohesion and adhesion with the aggregate, which prevent water from easily displacing bitumen from the aggregate surface, were responsible for the increase in the Marshall stability of the NESP-modified asphalt mixtures. This resulted from the increased reactivity between the NESP and the bitumen matrix, which is facilitated by the large surface area of NESP as the nanoparticles reinforce bitumen particles and improve their bonding [84]. Additionally, the adhesion improvement can be attributed to the increased surface free energy of the bitumen owing to the addition of NESP, which possesses alkaline characteristics owing to its high $CaCO_3$ content [48, 85]. These results agree with those obtained by Hao et al. [86], who noted that the addition of $CaCO_3$ nanoparticles to asphalt mixtures increases the Marshall stability.

Figure 15 shows the RSI results. The most notable improvement can be observed in the 9% NESP-modified asphalt mixture, which exhibits RSI values of 91.0 and 84.3% for immersion times of 24 and 48 h, respectively, whereas the 5% NESP-modified asphalt mixture exhibits RSI values of 90.5 and 83.7%, respectively. By contrast, the control mixture exhibits the lowest RSI values of 90.04% and 82.1% for immersion times of 24 and 48 h, respectively. This improvement can be attributed to the presence of NESP, which was uniformly distributed in the bitumen owing to its small size and large surface area, resulting in an increased structural bitumen ratio. Additionally, the high content of $CaCO_3$ in NESP reduces the acidity of bitumen, thereby enhancing its adhesion to granite aggregates [87].

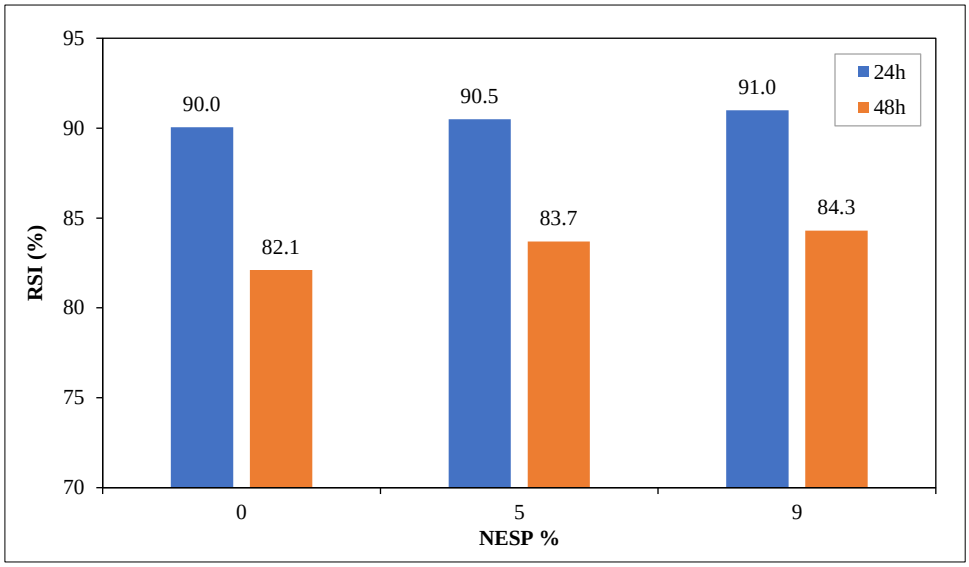

Figure 15. RSI results for samples immersed for 24 and 48 h

Figure 16 shows the durability index results, revealing that both the FDI and SDI values decreased as the NESP content increased. Specifically, the FDI values decreased by 9.0 and 11.0% for the 5% and 9% NESP-modified asphalt mixtures, respectively, compared with the control mixture. Similarly, the SDI values decreased by 10.7 and 16.4% for the 5 and 9% NESP-modified asphalt mixtures, respectively, compared with the control mixture. The durability index reflects the loss of strength or stability of an asphalt pavement. Therefore, a lower durability index value indicates lower strength and stability loss and therefore, higher durability [70]. Consequently, the addition of NESP enhanced the stability and durability of the asphalt mixtures under wet conditions.

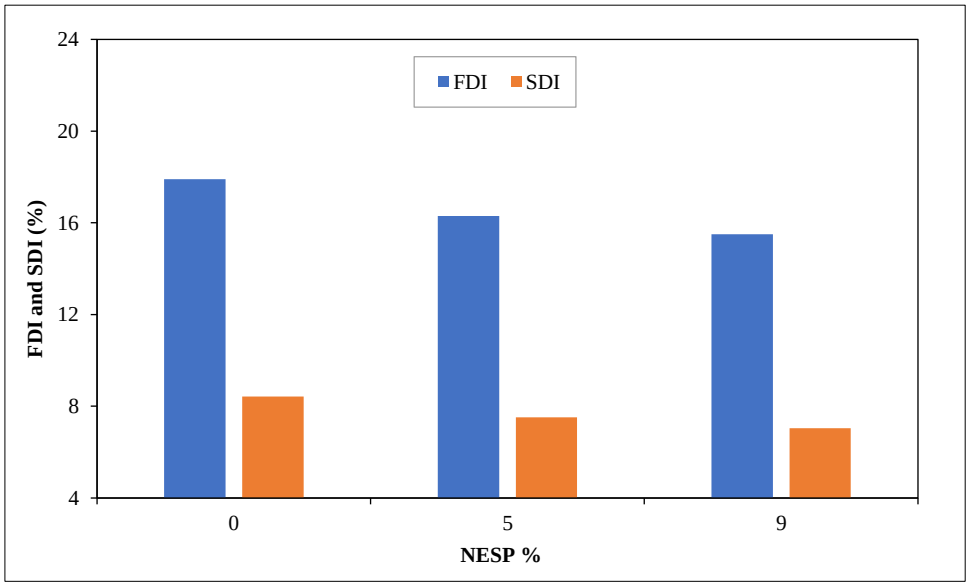

Figure 16. FDI and SDI results of samples immersed for 48 h

4.3. Resilient Modulus (Mr)

Figure 17 shows the Mr results of the three mixtures at 25 and 40 °C, which reflect their fatigue and rutting resistances, respectively. At both temperatures, the NESP-modified asphalt mixtures exhibited higher Mr values than the control mixture. At 25 °C, the control mixture exhibited the lowest Mr value of 2640 MPa, whereas the 5% and 9% NESP-modified asphalt mixtures exhibited Mr values of 2871 and 3397 MPa, respectively. The higher Mr values of the

NESP-modified asphalt mixtures suggest that they feature higher stiffness and elasticity, which allow them to return to their original states after the load is removed, thereby reducing fatigue cracking. This improvement can be attributed to the presence of NESP nanoparticles, which enhance the bitumen–aggregate adhesion. Additionally, nanomaterials improve the strength and elasticity of bitumen and are highly effective in controlling crack extensions [19]. Furthermore, the Mr results at 40°C exhibit a similar pattern. As anticipated, the Mr decreased at this temperature because bitumen softens and loses its elasticity at higher temperatures. Notably, the highest Mr of 731 MPa can be observed for the 9% NESP-modified asphalt mixture, followed by 653 MPa for the 5% NESP-modified asphalt mixture, whereas the control mixture exhibits the lowest Mr of 569 MPa. The higher Mr values of the NESP-modified asphalt mixtures at this temperature indicate their ability to resist permanent deformation or rutting. This can be attributed to the incorporation of NESP, which enhances the thermal properties of bitumen and prevents the degradation of its colloidal structure, thereby improving the elasticity of the asphalt mixture [88-90]. These findings align with those of previous studies, which found that bitumen modified with nano $CaCO_3$ enhanced the Mr of asphalt mixtures at medium and high temperatures [8, 91, 92].

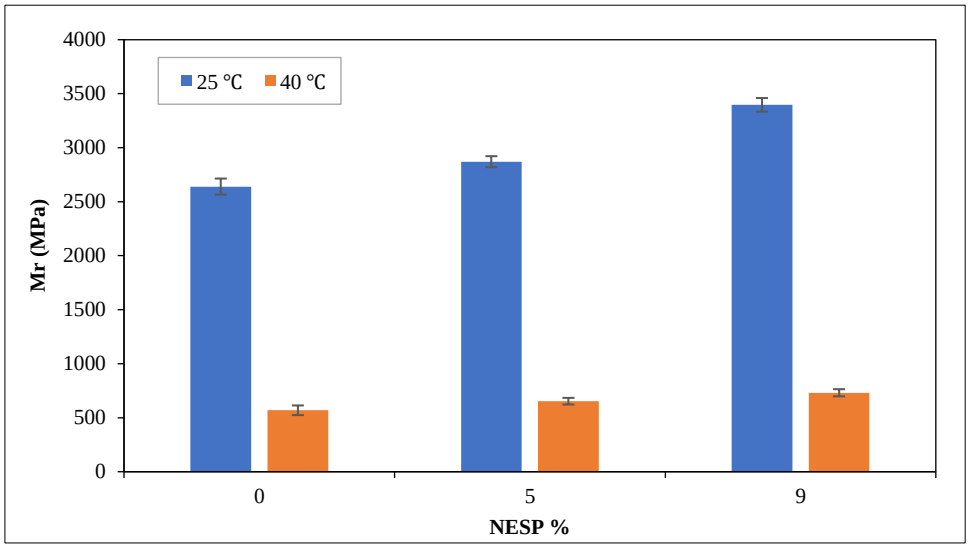

Figure 17. Mr results for the three mixtures at 25 and 40 °C

Figure 18 shows the recovered axial strain and total recoverable horizontal deformation of the control and NESP-modified asphalt mixtures. Notably, an opposite trend to that of the Mr is evident, indicating that a lower recovered axial strain led to higher Mr values of the mixtures. The recovered axial strain of the NESP-modified asphalt mixtures are lower than that of the control mixture at 25 °C, and similar trends are observed at 40 °C. Additionally, the recovered axial strains of the mixtures at 40 °C are greater than those at 25 °C. This can be attributed to the increase in temperature, which softens the bitumen and increases its deformation, leading to the greater deformation at 40 °C. However, the NESP-modified asphalt mixtures exhibited resistance to deformation, resulting in lower recoverable axial strains than that of the control mixture. These findings agree with the Mr results that demonstrated that the NESP-modified asphalt mixtures have higher Mr values.

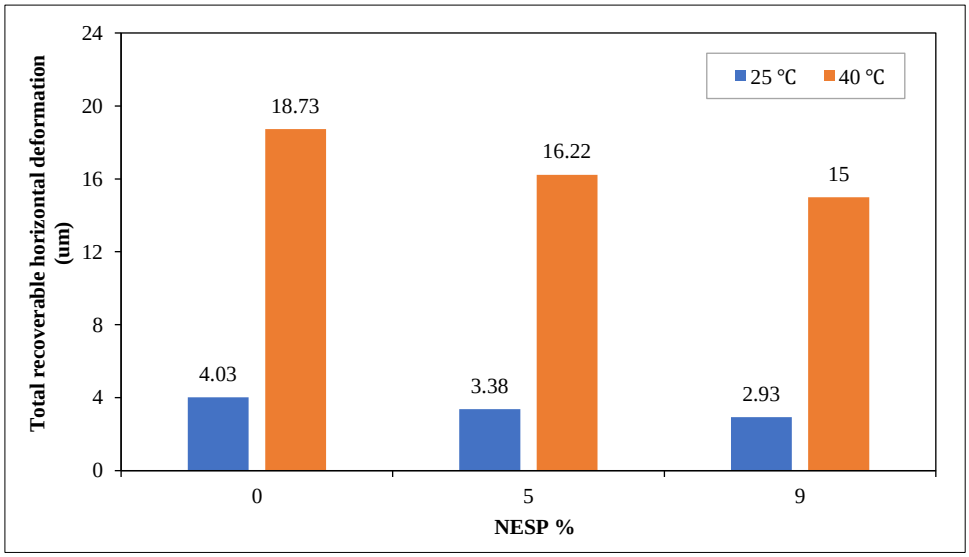

Figure 18. Total recoverable horizontal deformation (µm)

4.4. Dynamic Creep

Figure 19 shows the cumulative-strain results after 3600 cycles at 40°C, wherein the NESP-modified asphalt mixtures exhibit a lower permanent strain than the control mixture. The maximum permanent strain of the control mixture is 12542 microstrain, whereas those of the 5% and 9% NESP-modified asphalt mixtures are 11147 and 9318 microstrain, respectively. Thus, the permanent strain of the 9% NESP-modified asphalt mixture decreased by approximately 26% compared with the control mixture, indicating that NESP enhances resistance to permanent deformation and rutting. Figure 20 shows the values of the CSM and CSS, wherein the control, 5% NESP-modified asphalt, and 9% NESP-modified asphalt mixtures have creep stiffness values of 238, 268, and 310 MPa, respectively. Thus, the 9% NESP-modified asphalt mixture exhibited the most significant enhancement in creep stiffness, which can be attributed to the superior properties of the bitumen used in the mixture. The strong interfacial forces between the NESP particles and the bitumen matrix resulted in robust bonding and high adhesion of the bitumen [23], thereby enhancing the bitumen–aggregate bonding and leading to a notable improvement in the asphalt-mixture performance.

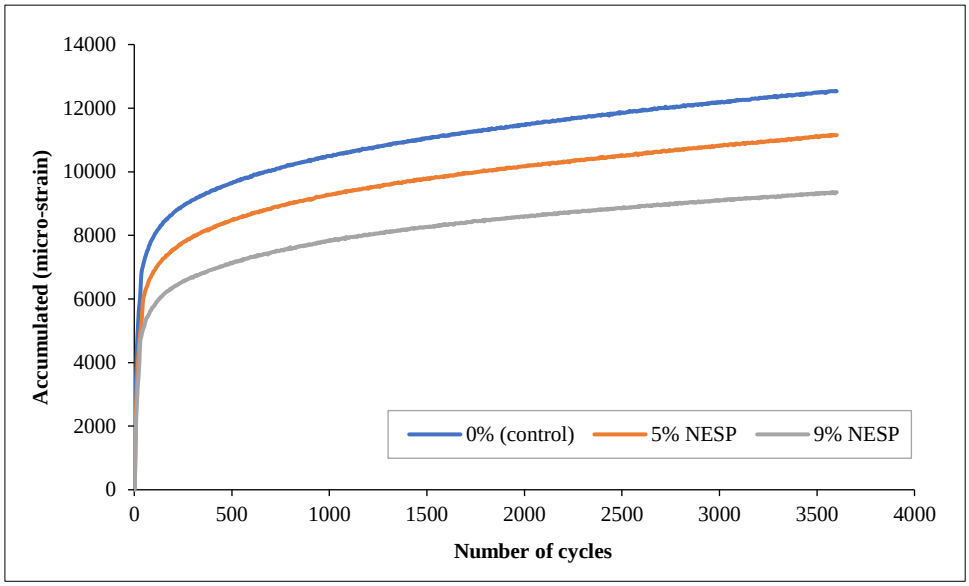

Figure 19. Cumulative-strain results of control and NESP-modified asphalt mixtures

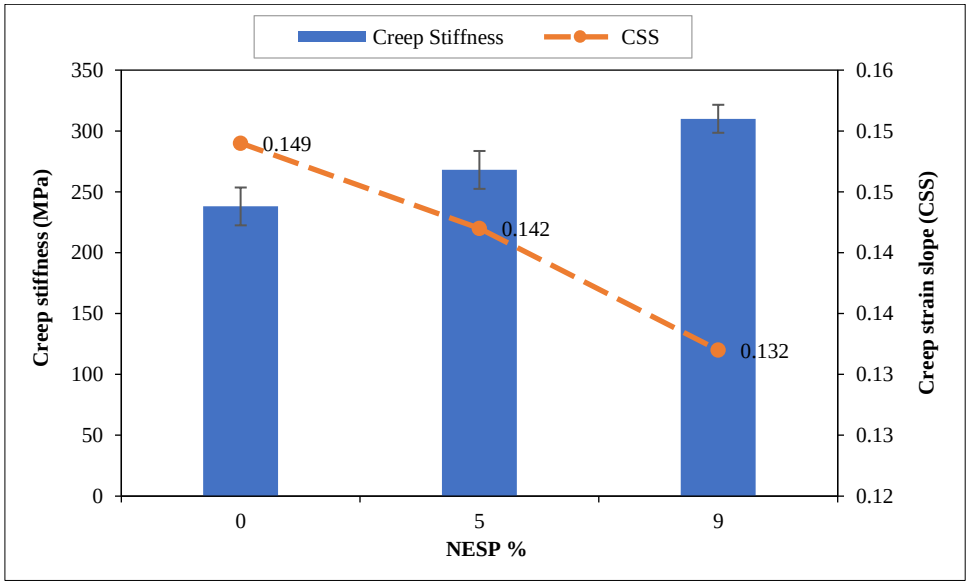

Figure 20. Creep-stiffness results and slopes of control and NESP-modified asphalt mixtures

To assess the resistance to permanent deformation during the initial phase, CSS was determined by calculating the slope of the permanent strain pattern from 1200–3600 cycles. As shown in Figure 20, the 9% NESP-modified asphalt mixture achieved the lowest CSS value of 0.132, whereas the 5% NESP-modified asphalt and control mixtures recorded values of 0.142 and 0.149, respectively. Lower CSS values indicate higher resistance to permanent deformation. Therefore, owing to their increased stiffness, the NESP-modified asphalt mixtures demonstrated greater resistance to

permanent deformation or rutting than the control mixture. Albayati et al. [92] also reported a similar finding, noting that asphalt mixtures containing bitumen modified with nano-$CaCO_3$ exhibit greater resistance to permanent deformation.

4.5. Double Punching (DP)

The DP test is an alternative method for assessing the rutting and fatigue resistance of asphalt mixtures [11, 93, 94]. The DP stress at 25 °C predicts the fatigue resistance of asphalt mixtures, with higher values indicating lower fatigue cracking. Additionally, the DP stress computed at 60 °C indicates the rutting resistance, with higher values suggesting lower rutting [11]. Figure 21 illustrates the DP stress results of the control and NESP-modified asphalt mixtures at 25 °C and 60 °C. A significant improvement in the DP stress of the mixtures with higher NESP content can be observed at 25 °C. Specifically, the 5% and 9% NESP-modified asphalt mixtures exhibit DP stress enhancements of 9% and 21%, respectively, compared with the control mixture. This indicates that the NESP-modified asphalt mixtures were significantly more resistant to fatigue cracking. This improvement can be attributed to the high surface area of NESP, which enhances the adhesion between bitumen particles and leads to the creation of a protective layer [48]. This layer plays a crucial role in absorbing the energy of the applied load, thereby delaying and mitigating crack occurrences [8].

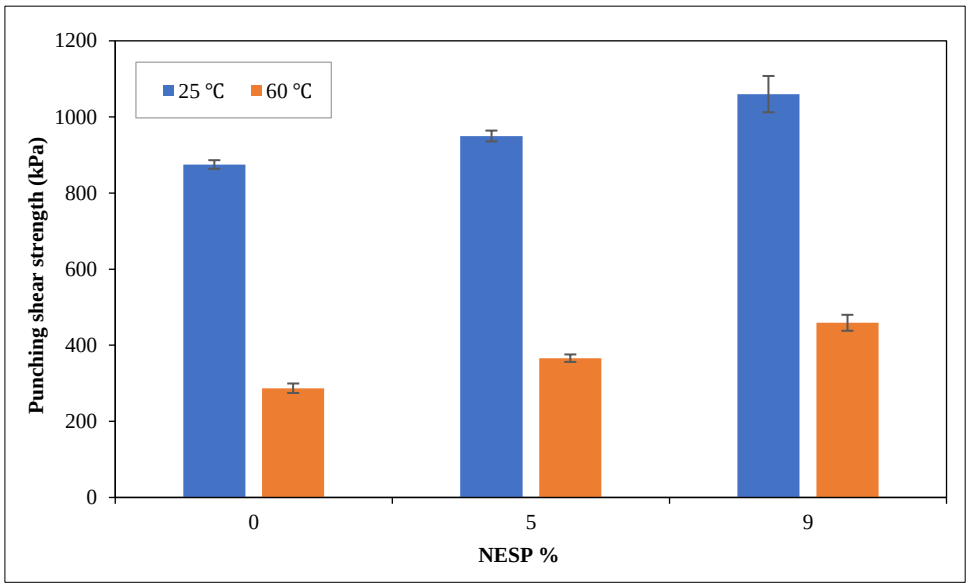

Figure 21. Punching shear strengths of the control and NESP-modified asphalt mixtures

Additionally, the results obtained at 60°C show that the addition of NESP enhances the strength of the asphalt mixture, with the 5% and 9% NESP-modified asphalt mixtures exhibiting 28.0% and 59.0% higher DP stress values, respectively, compared with the control mixture. This enhancement indicates the NESP-modified asphalt mixtures significantly improve the pavement's ability to withstand permanent deformation or rutting. The enhanced strength of the NESP-modified asphalt mixtures can be attributed to the improved properties of the bitumen film coating the aggregate. Additionally, the large surface area of NESP reinforces the bonds between the bitumen molecules and increases their adhesion and cohesion, which delays its transition from the elastic to viscous phase at higher temperatures [95].

4.6. Water Immersion

The loss of bitumen–aggregate adhesion owing to moisture significantly contributes to the failure of asphalt mixtures. Consequently, a water-immersion test was conducted to assess the stripping phenomenon and evaluate the bitumen–aggregate adhesion properties for both the control and NESP-modified asphalt mixtures. The results are shown in Figure 22, which demonstrates that ≥95% of aggregates were coated with bitumen after immersion, thereby meeting the specification limit set by the AASHTO T182 [76]. These findings indicate that as the NESP content increased, stripping reduced considerably, suggesting an enhancement of the bitumen–aggregate adhesion. The loss of adhesion can be attributed to the relatively acidic natures of both the bitumen and aggregates (granite), as they both tend to attract water particles [82, 96]. The addition of NESP, an alkaline material with high $CaCO_3$ content, increases the base component in the bitumen matrix. This enhances the reactivity between the aggregate and bitumen, resulting in improved adhesion and increased resistance to stripping [90]. This finding was also confirmed in a previous study, which noted that NESP enhances bitumen wettability [48]. Moreover, a previous study also obtained similar results, wherein the addition of nano-$CaCO_3$ to asphalt mixtures improved their stripping resistance [83, 97].

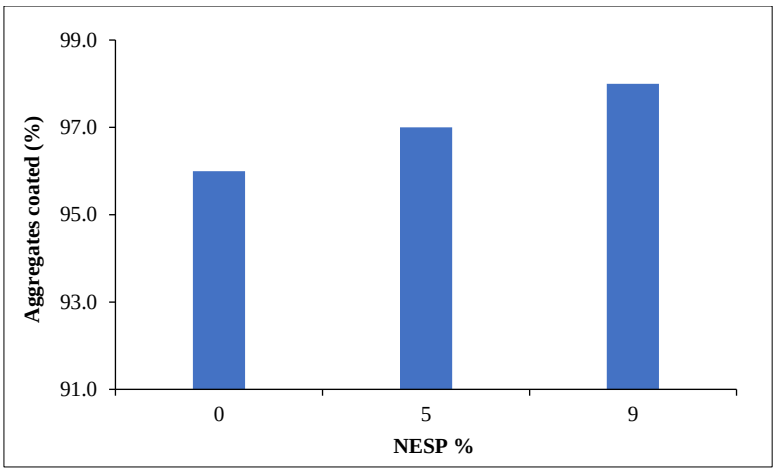

Figure 22. Water-immersion results for the control and NESP-modified asphalt mixtures

4.7. Wheel Tracking

The samples and results of both the control and NESP-modified asphalt mixtures after the wheel-tracking test at 60°C are shown in Figures 23-a and 23-b. Evidently, the 9% NESP-modified asphalt mixture exhibits the smallest rut depth of 3.72 mm, followed by the 5% NESP-modified asphalt mixture, which demonstrates a rut depth of 4.10 mm. By contrast, the control mixture exhibits a higher rut depth of 4.42 mm. This enhancement in rutting resistance of asphalt mixtures can be attributed to the bitumen used in them [98]. At high temperatures and under repeated loading, the bitumen layer binding the aggregate structure becomes softer and thinner, and its colloidal structure becomes less cohesive. NESP can mitigate these disruptions to the colloidal composition owing to its high surface area, which allows it to interact strongly with the oily components of bitumen. This interaction leads to the conversion of the colloidal bitumen system from sol to gel, resulting in significant increases in viscosity and adhesion [48, 84]. This enhancement can also be attributed to an increase in the rutting parameter (G*/sin δ) of bitumen through the addition of NESP [48]. However, all mixtures exhibited rut depths of <8 mm, which is in accordance with the specifications of asphalt-mix performance outlined by the Virginia Department of Transportation (VDOT) [99]. Additionally, these findings align with those of Manfro et al. [59], who noted that the addition of nano-$CaCO_3$ to asphalt mixtures enhances their resistance to permanent deformation and rutting.

(a)

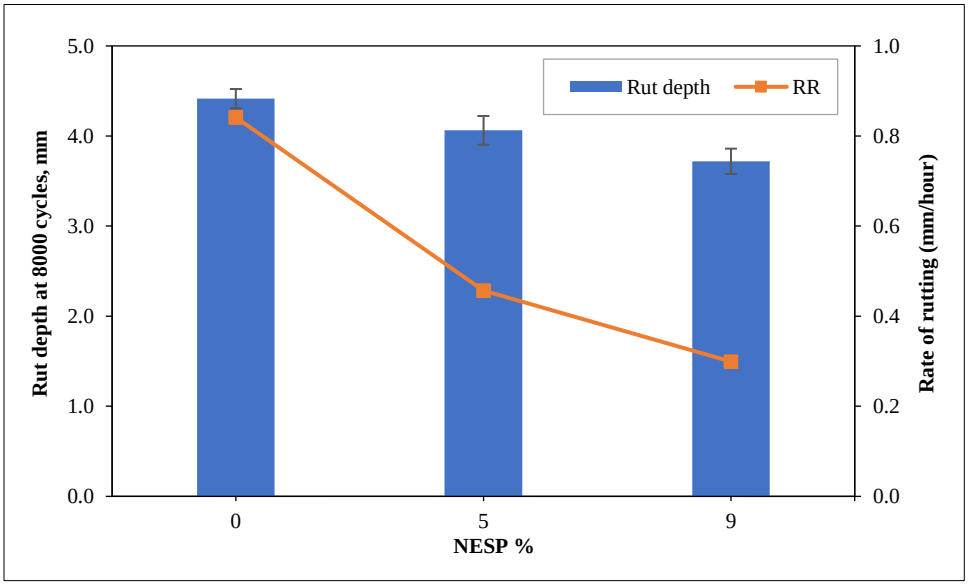

(b)

Figure 23. a) Samples of control and NESP-modified asphalt mixtures; b) rut depths and RRs after wheel-tracking test at 60 ℃

The RR results in Figure 23-b indicate that mixtures with higher NESP content exhibit lower RRs, which indicate their enhanced resistance to permanent deformation [79, 80]. Specifically, the control mixture exhibits the highest RR of 0.84 mm/h, whereas the 9% NESP-modified asphalt mixture exhibits the lowest RR of 0.30 mm/h. These findings indicate that incorporating NESP reduces permanent deformation or rutting and provide additional evidence that the addition of NESP can increase the rutting resistance of asphalt mixtures.

5. Conclusion

This study investigated the effects of NESP on the mechanical properties of asphalt mixtures. Mechanical tests conducted on both the control and 5% and 9% NESP-modified asphalt mixtures revealed that the addition of NESP enhanced the moisture resistance of the mixtures by increasing their TSR. Furthermore, the modified mixtures exhibited better durability, as indicated by their lower FDI and SDI values and higher RSI values. Moreover, the NESP-modified mixtures exhibited higher Mr values at 25 and 40 °C than the control mixture. Additionally, NESP increased the CSM of the asphalt mixtures and reduced their permanent deformation. The results of the DP shear tests indicated that asphalt mixtures with higher NESP content exhibited better rutting and fatigue resistances. The incorporation of NESP also enhanced the bitumen–aggregate adhesion, thereby increasing the resistance of the mixtures to stripping. Finally, the wheel-tracking results confirmed that the NESP-modified mixtures exhibited lower rut depths than the control mixture. Additionally, 9% NESP content was determined to be optimal for enhancing the mechanical properties of asphalt mixtures. These findings demonstrate that NESP has several potential environmental benefits, including waste reduction and improved pavement performance, leading to longer service life and reduced maintenance costs.

Future studies should experiment with asphalt mixtures incorporating more than 9% NESP to further optimize their performance and identify the best NESP to bitumen ratio. Additionally, field tests should be conducted to evaluate the performance of asphalt mixtures containing NESP-modified bitumen, particularly for maintenance applications. It is also recommended to investigate the potential of other biomaterial wastes as nanomaterials for bitumen modification, which could contribute to mitigating the environmental effects of these waste materials and enhance their recycling.

6. Declarations

6.1. Author Contributions

Conceptualization, N.H.M.K., R.P.J., H.Y., and Z.H.A.; methodology, N.H.M.K., R.P.J., H.Y., and Z.H.A.; writing—original draft preparation, A.H.Z.C.; writing—review and editing, H.Y. and Z.H.A.; visualization, N.H.M.K. and R.P.J. All authors have read and agreed to the published version of the manuscript.

6.2. Data Availability Statement

The data presented in this study are available on request from the corresponding author.

6.3. Funding

The authors received no financial support for the research, authorship, or publication of this manuscript.

6.4. Acknowledgements

We wish to acknowledge the Universiti Teknologi Malaysia for providing support and resources for this research. We would also like to extend our gratitude to all the technicians in the highway and transportation laboratories at the UTM and UTHM Universities for their assistance and cooperation.

6.5. Conflicts of Interest

The authors declare no conflict of interest.

7. References

[1] Kharissova, A. B., Kharissova, O. V., Kharisov, B. I., & Méndez, Y. P. (2024). Carbon negative footprint materials: A review. Nano-Structures & Nano-Objects, 37, 101100. doi:10.1016/j.nanoso.2024.101100.

[2] Pata, U. K., Kartal, M. T., & Mukhtarov, S. (2024). Technological changes and carbon neutrality targets in European countries: A sustainability approach with Fourier approximations. Technological Forecasting and Social Change, 198, 122994. doi:10.1016/j.techfore.2023.122994.

[3] Wang, X., Ji, G., Zhang, Y., Guo, Y., & Zhao, J. (2021). Research on high-and low-temperature characteristics of bitumen blended with waste eggshell powder. Materials, 14(8). doi:10.3390/ma14082020.

[4] Debbarma, K., Debnath, B., & Sarkar, P. P. (2022). A comprehensive review on the usage of nanomaterials in asphalt mixes. Construction and Building Materials, 361, 129634. doi:10.1016/j.conbuildmat.2022.129634.

[5] Kamboozia, N., Saed, S. A., & Rad, S. M. (2021). Rheological behavior of asphalt binders and fatigue resistance of SMA mixtures modified with nano-silica containing RAP materials under the effect of mixture conditioning. Construction and Building Materials, 303, 124433. doi:10.1016/j.conbuildmat.2021.124433.

[6] Das, A. K., & Singh, D. (2021). Evaluation of fatigue performance of asphalt mastics composed of nano hydrated lime filler. Construction and Building Materials, 269, 121322. doi:10.1016/j.conbuildmat.2020.121322.

[7] Aljbouri, H. J., & Albayati, A. H. (2023). Effect of nanomaterials on the durability of hot mix asphalt. Transportation Engineering, 11, 100165. doi:10.1016/j.treng.2023.100165.

[8] Yarahmadi, A. M., Shafabakhsh, G., & Asakereh, A. (2022). Laboratory investigation of the effect of nano Caco3 on rutting and fatigue of stone mastic asphalt mixtures. Construction and Building Materials, 317, 126127. doi:10.1016/j.conbuildmat.2021.126127.

[9] Li, H., Liu, S., Yang, F., He, S., Jing, H., Zou, X., Li, Z., & Sheng, Y. (2024). Review of utilization of bamboo fiber in asphalt modification: Insights into preparation, performance, reinforcement, and challenges. Journal of Cleaner Production, 468, 143010. doi:10.1016/j.jclepro.2024.143010.

[10] Al-Hadidy, A. I. (2024). Experimental Investigation on Performance of Asphalt Mixtures with Waste Materials. International Journal of Pavement Research and Technology, 17(4), 1079–1091. doi:10.1007/s42947-023-00288-w.

[11] Aboelmagd, A., Moussa, G., Enieb, M., Khedr, S., & Abd Alla, E.-S. (2021). Evaluation of Hot Mix Asphalt and Binder Performance Modified With High Content of Nano Silica Fume. Journal of Engineering Sciences, 49(4), 1–22. doi:10.21608/jesaun.2021.70733.1046.

[12] Broering, W. B., de Melo, J. V. S., & Manfro, A. L. (2022). Incorporation of nanoalumina into a polymeric asphalt matrix: Reinforcement of the nanostructure, improvement of phase stability, and amplification of rheological parameters. Construction and Building Materials, 320, 126261. doi:10.1016/j.conbuildmat.2021.126261.

[13] Zhu, J., Birgisson, B., & Kringos, N. (2014). Polymer modification of bitumen: Advances and challenges. European Polymer Journal, 54(1), 18–38. doi:10.1016/j.eurpolymj.2014.02.005.

[14] Fang, C., Yu, R., Liu, S., & Li, Y. (2013). Nanomaterials applied in asphalt modification: A review. Journal of Materials Science & Technology, 29(7), 589–594. doi:10.1016/j.jmst.2013.04.008.

[15] Alghrafy, Y. M., Abd Alla, E. S. M., & El-Badawy, S. M. (2021). Phase angle master curves of sulfur-extended asphalt modified with recycled polyethylene waste. Innovative Infrastructure Solutions, 6(2), 1–11. doi:10.1007/s41062-021-00459-3.

[16] Ji, Z., Sun, L., Chen, L., Gu, W., Tian, Y., & Zhang, X. (2023). Pavement performance and modification mechanisms of asphalt binder with nano-Al_2O_3. International Journal of Pavement Engineering, 24(2), 2136373. doi:10.1080/10298436.2022.2136373.

[17] Ali Shafabakhsh, G., Sadeghneja, M., & Alizadeh, S. (2023). Engineering the Effect of Nanomaterials on Bitumen and Asphalt Mixture Properties. A Review. The Baltic Journal of Road and Bridge Engineering, 18(2), 1–31. doi:10.7250/bjrbe.2023-18.596.

[18] Alam, M. R., Safiuddin, M., Collins, C. M., Hossain, K., & Bazan, C. (2024). Innovative use of nanomaterials for improving performance of asphalt binder and asphaltic concrete: a state-of-the-art review. International Journal of Pavement Engineering, 25(1), 2370567. doi:10.1080/10298436.2024.2370567.

[19] Bhat, F. S., Gilani, T. A., Din, I. M. U., Aziz, G., Mir, M. S., Shah, A. H., Sheikh, I. R., & Mudasir, P. (2024). Integration of nano Al2O3 and nano SiO2 in asphalt mixes: A comprehensive performance and durability evaluation. Construction and Building Materials, 412, 134687. doi:10.1016/j.conbuildmat.2023.134687.

[20] Abdel-Wahed, T., Abdel-Raheem, A., & Moussa, G. (2022). Performance Evaluation of Asphalt Mixtures Modified with Nanomaterials. (Dept. C). Mansoura Engineering Journal, 47(1), 1–15. doi:10.21608/bfemu.2022.221670.

[21] Hussein, A. A., Jaya, R. P., Abdul Hassan, N., Yaacob, H., Huseien, G. F., & Ibrahim, M. H. W. (2017). Performance of nanoceramic powder on the chemical and physical properties of bitumen. Construction and Building Materials, 156, 496–505. doi:10.1016/j.conbuildmat.2017.09.014.

[22] Johnson, T. W., Hashemian, L., Patra, S., & Shabani, A. (2019, September). Application of nanoclay materials in asphalt pavements. Joint Conference and Exhibition of the Transportation Association of Canada, TAC and Intelligent Transportation Systems Canada, ITSC, 22-25 September 2019, Halifax, Canada.

[23] Jeffry, S. N. A., Jaya, R. P., Abdul Hassan, N., Yaacob, H., & Satar, M. K. I. M. (2018). Mechanical performance of asphalt mixture containing nano-charcoal coconut shell ash. Construction and Building Materials, 173, 40–48. doi:10.1016/j.conbuildmat.2018.04.024.

[24] Ashish, P. K., & Singh, D. (2019). Effect of Carbon Nano Tube on performance of asphalt binder under creep-recovery and sustained loading conditions. Construction and Building Materials, 215, 523–543. doi:10.1016/j.conbuildmat.2019.04.199.

[25] Lv, S., Xia, C., Yang, Q., Guo, S., You, L., Guo, Y., & Zheng, J. (2020). Improvements on high-temperature stability, rheology, and stiffness of asphalt binder modified with waste crayfish shell powder. Journal of Cleaner Production, 264, 121745. doi:10.1016/j.jclepro.2020.121745.

[26] Yang, X., Mills-Beale, J., & You, Z. (2017). Chemical characterization and oxidative aging of bio-asphalt and its compatibility with petroleum asphalt. Journal of Cleaner Production, 142, 1837–1847. doi:10.1016/j.jclepro.2016.11.100.

[27] Sathvik, S., Kumar, G. S., Bahrami, A., Nitin, G. C., Singh, S. K., Althaqafi, E., & Özkılıç, Y. O. (2024). Evaluation of asphalt binder and mixture properties utilizing fish scale powder as a biomodifier. Case Studies in Construction Materials, 20, 3238. doi:10.1016/j.cscm.2024.e03238.

[28] Huang, J., Shiva Kumar, G., Ren, J., Sun, Y., Li, Y., & Wang, C. (2022). Towards the potential usage of eggshell powder as bio-modifier for asphalt binder and mixture: workability and mechanical properties. International Journal of Pavement Engineering, 23(10), 3553–3565. doi:10.1080/10298436.2021.1905809.

[29] Fan, G., Liu, H., Liu, C., Xue, Y., Ju, Z., Ding, S., Zhang, Y., & Li, Y. (2022). Analysis of the Influence of Waste Seashell as Modified Materials on Asphalt Pavement Performance. Materials, 15(19), 6788. doi:10.3390/ma15196788.

[30] Guo, Y., Wang, X., Ji, G., Zhang, Y., Su, H., & Luo, Y. (2021). Effect of recycled shell waste as a modifier on the high-and low-temperature rheological properties of asphalt. Sustainability (Switzerland), 13(18), 271. doi:10.3390/su131810271.

[31] Hu, C., Zhong, D., & Li, S. (2023). A study on effect of oyster shell powder on mechanical properties of asphalt and multiple degrees of modification mechanism. Case Studies in Construction Materials, 18, 1786. doi:10.1016/j.cscm.2022.e01786.

[32] Ali Said Al Abri, S., Rahul Rollakanti, C., Kumar Poloju, K., & Joe, A. (2022). Experimental Study on Mechanical Properties of Concrete by partial replacement of Cement with Eggshell Powder for Sustainable Construction. Materials Today: Proceedings, 65, 1660–1665. doi:10.1016/j.matpr.2022.04.708.

[33] Alsharari, F., Khan, K., Amin, M. N., Ahmad, W., Khan, U., Mutnbak, M., Houda, M., & Yosri, A. M. (2022). Sustainable use of waste eggshells in cementitious materials: An experimental and modeling-based study. Case Studies in Construction Materials, 17, 1620. doi:10.1016/j.cscm.2022.e01620.

[34] Waheed, M., Yousaf, M., Shehzad, A., Inam-Ur-Raheem, M., Khan, M. K. I., Khan, M. R., Ahmad, N., Abdullah, & Aadil, R. M. (2020). Channelling eggshell waste to valuable and utilizable products: A comprehensive review. Trends in Food Science and Technology, 106, 78–90. doi:10.1016/j.tifs.2020.10.009.

[35] Francis, A. A., & Abdel Rahman, M. K. (2016). The environmental sustainability of calcined calcium phosphates production from the milling of eggshell wastes and phosphoric acid. Journal of Cleaner Production, 137, 1432–1438. doi:10.1016/j.jclepro.2016.08.029.

[36] Khan, K., Ahmad, W., Amin, M. N., & Deifalla, A. F. (2023). Investigating the feasibility of using waste eggshells in cement-based materials for sustainable construction. Journal of Materials Research and Technology, 23, 4059–4074. doi:10.1016/j.jmrt.2023.02.057.

[37] Shekhawat, P., Sharma, G., & Singh, R. M. (2019). Strength behavior of alkaline activated eggshell powder and flyash geopolymer cured at ambient temperature. Construction and Building Materials, 223, 1112–1122. doi:10.1016/j.conbuildmat.2019.07.325.

[38] Thaha, A. H., Malaka, R., Hatta, W., & Maruddin, F. (2024). Staphylococcus aureus as a foodborne pathogen in eggs and egg products in Indonesia: A review. International Journal of One Health, 10(1), 141–147. doi:10.14202/IJOH.2023.141-147.

[39] Owuamanam, S., & Cree, D. (2020). Progress of bio-calcium carbonate waste eggshell and seashell fillers in polymer composites: A review. Journal of Composites Science, 4(2), 70. doi:10.3390/jcs4020070.

[40] Zhang, Y., Chen, Y., Kang, Z. W., Gao, X., Zeng, X., Liu, M., & Yang, D. P. (2021). Waste eggshell membrane-assisted synthesis of magnetic $CuFe_2O_4$ nanomaterials with multifunctional properties (adsorptive, catalytic, antibacterial) for water remediation. Colloids and Surfaces A: Physicochemical and Engineering Aspects, 612, 125874. doi:10.1016/j.colsurfa.2020.125874.

[41] Amin, M., Attia, M. M., Agwa, I. S., Elsakhawy, Y., el-hassan, K. A., & Abdelsalam, B. A. (2022). Effects of sugarcane bagasse ash and nano eggshell powder on high-strength concrete properties. Case Studies in Construction Materials, 17, 1528. doi:10.1016/j.cscm.2022.e01528.

[42] Ismael, E., Fahim, K. M., Ghorab, S. M. O., Hamouda, R. H., Rady, A. M., Zaki, M. M., & Gamal, A. M. (2024). Sustainable recycling of poultry eggshell waste for the synthesis of calcium oxide nanoparticles and evaluating its antibacterial potency against food-borne pathogens. Journal of Advanced Veterinary Research, 14(1), 130–134.

[43] Lee, M., Tsai, W. S., & Chen, S. T. (2020). Reusing shell waste as a soil conditioner alternative? A comparative study of eggshell and oyster shell using a life cycle assessment approach. Journal of Cleaner Production, 265, 121845. doi:10.1016/j.jclepro.2020.121845.

[44] Ferraz, E., Gamelas, J. A. F., Coroado, J., Monteiro, C., & Rocha, F. (2018). Eggshell waste to produce building lime: calcium oxide reactivity, industrial, environmental and economic implications. Materials and Structures, 51(5), 115. doi:10.1617/s11527-018-1243-7.

[45] Liu, Q., Zeng, J., Chen, S., He, X., Su, Y., Hu, S., Yang, C., & Zheng, G. (2024). Enhancement of bitumen aging resistance by nanomicron porous eggshell loaded with waste engine oil prepared under mechanical force. Construction and Building Materials, 438, 137101. doi:10.1016/j.conbuildmat.2024.137101.

[46] Masri, K. A., Ganesan, E., Ramadhansyah, P. J., Doh, S. I., Jasni, N. E., Al-Saffar, Z. H., & Mohammed, A. A. (2021). Volumetric Properties and Abrasion Resistance of Stone Mastic Asphalt Incorporating Eggshell Powder. IOP Conference Series: Earth and Environmental Science, 682(1). doi:10.1088/1755-1315/682/1/012058.

[47] Zani, L., Giustozzi, F., & Harvey, J. (2017). Effect of storage stability on chemical and rheological properties of polymer-modified asphalt binders for road pavement construction. Construction and Building Materials, 145, 326–335. doi:10.1016/j.conbuildmat.2017.04.014.

[48] Zghair Chfat, A. H., Yaacob, H., Mohd Kamaruddin, N. H., Al-Saffar, Z. H., & Putra Jaya, R. (2024). Effects of nano eggshell powder as a sustainable bio-filler on the physical, rheological, and microstructure properties of bitumen. Results in Engineering, 22, 102061. doi:10.1016/j.rineng.2024.102061.

[49] Jabatan Kerja Raya (JKR). (2008). Standard Specification for Road Works-Section 4: Flexible Pavement, Jabatan Kerja Raya Malaysia, Kuala Lumpur, Malaysia.

[50] ASTM D5-06. (2017). Standard Test Method for Penetration of Bituminous Materials. ASTM International, Pennsylvania, United States. doi:10.1520/D0005-06.

[51] ASTM D36/D36M-12. (2014). Standard Test Method for Softening Point of Bitumen (Ring-and-Ball Apparatus). ASTM International, Pennsylvania, United States. doi:10.1520/D0036_D0036M-12.

[52] ASTM D4402/D4402M-15 (2022). Standard Test Method for Viscosity Determination of Asphalt at Elevated Temperatures Using a Rotational Viscometer. ASTM International, Pennsylvania, United States. doi:10.1520/D4402_D4402M-15.

[53] ASTM D7175-15. (2024). Standard Test Method for Determining the Rheological Properties of Asphalt Binder Using a Dynamic Shear Rheometer. ASTM International, Pennsylvania, United States. doi:10.1520/D7175-15.

[54] ASTM C127-24. (2024). Standard Test Method for Relative Density (Specific Gravity) and Absorption of Coarse Aggregate. ASTM International, Pennsylvania, United States. doi:10.1520/C0127-24.

[55] ASTM C128-07a. (2012). Standard Test Method for Density, Relative Density (Specific Gravity), and Absorption of Fine Aggregate. ASTM International, Pennsylvania, United States. doi:10.1520/C0128-07A.

[56] BS EN 1097-2. (2020). Tests for Mechanical and Physical Properties of Aggregates-Part 2: Methods for the Determination of Resistance to Fragmentation. British Standards Institution (BSI), London, United Kingdom.

[57] BS EN 933-3. (2012). Tests for Geometrical Properties of Aggregates-Part 3: Determination of particle shape-Flakiness index. British Standards Institution (BSI), London, United Kingdom.

[58] BS EN 933-4. (2012). Tests for Geometrical Properties of Aggregates-Part 4: Determination of Particle shape-Shape index. British Standards Institution (BSI), London, United Kingdom.

[59] Manfro, A. L., Staub de Melo, J. V., Villena Del Carpio, J. A., & Broering, W. B. (2022). Permanent deformation performance under moisture effect of an asphalt mixture modified by calcium carbonate nanoparticles. Construction and Building Materials, 342, 128087. doi:10.1016/j.conbuildmat.2022.128087.

[60] Nazari, H., Naderi, K., & Moghadas Nejad, F. (2018). Improving aging resistance and fatigue performance of asphalt binders using inorganic nanoparticles. Construction and Building Materials, 170, 591–602. doi:10.1016/j.conbuildmat.2018.03.107.

[61] Ghasemzadeh Mahani, A., Bazoobandi, P., Hosseinian, S. M., & Ziari, H. (2021). Experimental investigation and multi-objective optimization of fracture properties of asphalt mixtures containing nano-calcium carbonate. Construction and Building Materials, 285, 122876. doi:10.1016/j.conbuildmat.2021.122876.

[62] Razavi, S. H., & Kavussi, A. (2020). The role of nanomaterials in reducing moisture damage of asphalt mixes. Construction and Building Materials, 239, 117827. doi:10.1016/j.conbuildmat.2019.117827.

[63] ASTM D6927-15. (2022). Standard Test Method for Marshall Stability and Flow of Asphalt Mixtures. ASTM International, Pennsylvania, United States. doi:10.1520/D6927-15.

[64] Kök, B. V., & Çolak, H. (2011). Laboratory comparison of the crumb-rubber and SBS modified bitumen and hot mix asphalt. Construction and Building Materials, 25(8), 3204–3212. doi:10.1016/j.conbuildmat.2011.03.005.

[65] Ameri, M., Mansourian, A., & Sheikhmotevali, A. H. (2013). Laboratory evaluation of ethylene vinyl acetate modified bitumens and mixtures based upon performance related parameters. Construction and Building Materials, 40, 438–447. doi:10.1016/j.conbuildmat.2012.09.109.

[66] Rodrigues, Y. O., da Silva, D. B., de Figueirêdo Lopes Lucena, L. C., & Lopes, M. C. (2017). Performance of warm mix asphalt containing Moringa oleifera Lam seeds oil: Rheological and mechanical properties. Construction and Building Materials, 154, 137–143. doi:10.1016/j.conbuildmat.2017.07.194.

[67] ASTM D4867/D4867M-09(2014). (2022). Standard Test Method for Effect of Moisture on Asphalt Concrete Paving Mixtures. ASTM International, Pennsylvania, United States. doi:10.1520/D4867_D4867M-09R14.

[68] ASTM D1075-07. (2011). Standard Test Method for Effect of Water on Compressive Strength of Compacted Bituminous Mixtures. ASTM International, Pennsylvania, United States. doi:10.1520/D1075-07.

[69] Putri, E. E., & Sari, R. R. (2021). The study of split mastic asphalt pavement with latex addition for flooded road. IOP Conference Series: Earth and Environmental Science, 708(1). doi:10.1088/1755-1315/708/1/012046.

[70] Kurnia, A. Y., Dewi, R., Permata, D. Y., Pataras, M., & Adelia, S. (2020). Characteristics Comparison of Refinery Asphalt, Rubberized Asphalt, and Buton Asphalt in Stone Matrix Asphalt Pavement with Marshall and Cantabro Method. Journal of Physics: Conference Series, 1500(1). doi:10.1088/1742-6596/1500/1/012125.

[71] ASTM D7369-20. (2020). Standard Test Method for Determining the Resilient Modulus of Asphalt Mixtures by Indirect Tension Test. ASTM International, Pennsylvania, United States. doi:10.1520/D7369-20.

[72] BS EN 12697-25. (2013). Bituminous Mixtures – Test Methods for Hot Mix Asphalt Part 25: Cyclic Compression Test. British Standards Institution (BSI), London, United Kingdom.

[73] Kareem, M. A., Al-Jumaili, M. A., & Kareem, Y. N. A. (2023). Evaluating of Plastic Bottle Waste on Moisture Damage of Asphalt Concrete Mixture. AIP Conference Proceedings, 2775(1). doi:10.1063/5.0141586.

[74] Hamdan, R. K., & Sarsam, S. I. (2019). Impact of Rejuvenators Type on Physical Properties of Aged Asphalt Cement. Civil Engineering Journal (Iran), 5(9), 2058–2069. doi:10.28991/cej-2019-03091393.

[75] Khalil, S. mahmood, & Sarsam, S. I. (2020). Influence of fly ash on the volumetric and physical properties of Stone Matrix Asphalt Concrete. Journal of Engineering, 26(5), 128–142. doi:10.31026/j.eng.2020.05.09.

[76] AASHTO T182. (2002). Standard method of test for coating and stripping of bitumen-aggregate mixtures. AASHTO Standards, Washington, United States.

[77] Mohd Jakarni, F., Rosli, M. F., Md Yusoff, N. I., Aziz, M. M. A., Muniandy, R., & Hassim, S. (2016). An overview of moisture damage performance tests on asphalt mixtures. Jurnal Teknologi, 78(7–2), 91–98. doi:10.11113/jt.v78.9497.

[78] AASHTO TP 63-03. (2003). Standard Method of Testing for Determining Rutting Susceptibility of Hot Mix Asphalt Using the Asphalt Pavement Analyzer. AASHTO Standards, Washington, United States.

[79] Ai, A. H., Yi-Qiu, T., & Hameed, A. T. (2011). Starch as a modifier for asphalt paving materials. Construction and Building Materials, 25(1), 14–20. doi:10.1016/j.conbuildmat.2010.06.062.

[80] Al-Hadidy, A. I. (2020). Performance of SBS-HMA Mixes Made with Sasobit and Zeolite. Journal of Materials in Civil Engineering, 32(10), 6020017. doi:10.1061/(asce)mt.1943-5533.0003362.

[81] Cong, P., Chen, Z., & Ge, W. (2023). Influence of moisture on the migration of asphalt components and the adhesion between asphalt binder and aggregate. Construction and Building Materials, 385, 131513. doi:10.1016/j.conbuildmat.2023.131513.

[82] Hamedi, G. H., Moghadas Nejad, F., & Oveisi, K. (2015). Investigating the effects of using nanomaterials on moisture damage of HMA. Road Materials and Pavement Design, 16(3), 536–552. doi:10.1080/14680629.2015.1020850.

[83] Hamedi, G. H., & Moghadas Nejad, F. (2024). Moisture Sensitivity of Hot Mix Asphalt Modified with Micronized Calcium Carbonate. Periodica Polytechnica Civil Engineering. doi:10.3311/ppci.23201.

[84] Sadeghnejad, M., & Shafabakhsh, G. (2017). Use of Nano SiO2 and Nano TiO2 to improve the mechanical behaviour of stone mastic asphalt mixtures. Construction and Building Materials, 157, 965–974. doi:10.1016/j.conbuildmat.2017.09.163.

[85] Sadeghnejad, M., & Shafabakhsh, G. (2017). Estimation the Fatigue Number of Stone Mastic Asphalt Mixtures Modified with Nano SiO2 and Nano TiO2. Journal of Rehabilitation in Civil Engineering, 5(1), 17–32. doi:10.22075/jrce.2017.1835.1158.

[86] Hao, X., Wang, Y., & Zhang, A. (2018). Research and Mechanism Analysis on Improving the Performance of Granite Asphalt Mixture. IOP Conference Series: Earth and Environmental Science, 189(3). doi:10.1088/1755-1315/189/3/032055.

[87] Hamedi, G. H., & Moghadas Nejad, F. (2016). Use of aggregate nanocoating to decrease moisture damage of hot mix asphalt. Road Materials and Pavement Design, 17(1), 32–51. doi:10.1080/14680629.2015.1056215.

[88] Yang, Q., Liu, Q., Zhong, J., Hong, B., Wang, D., & Oeser, M. (2019). Rheological and micro-structural characterization of bitumen modified with carbon nanomaterials. Construction and Building Materials, 201, 580–589. doi:10.1016/j.conbuildmat.2018.12.173.

[89] Chen, Z., Zhang, H., Zhu, C., & Zhao, B. (2015). Rheological examination of aging in bitumen with inorganic nanoparticles and organic expanded vermiculite. Construction and Building Materials, 101, 884–891. doi:10.1016/j.conbuildmat.2015.10.153.

[90] Hao, X., Wang, Y., & Zhang, A. (2014). A study on improving the adhesiveness between granite and asphalt by nano-scaled calcium carbonate. Key Engineering Materials, 575–576, 54–57. doi:10.4028/www.scientific.net/KEM.575-576.54.

[91] Omrani, M., & Babagoli, R. (2023). Evaluation of the Effect of Nano-Calcium Carbonate Mechanical Performance of Asphalt Binder and Mixture. Journal of Transportation Research, 20(3), 467-488.

[92] Albayati, A. H., Al-Ani, A. F., Byzyka, J., Al-Kheetan, M., & Rahman, M. (2024). Enhancing Asphalt Performance and Its Long-Term Sustainability with Nano Calcium Carbonate and Nano Hydrated Lime. Sustainability (Switzerland), 16(4), 1507. doi:10.3390/su16041507.

[93] Walubita, L. F., Faruk, A. N. M., Fuentes, L., Prakoso, A., Dessouky, S., Naik, B., & Nyamuhokya, T. (2019). Using the Simple Punching Shear Test (SPST) for evaluating the HMA shear properties and predicting field rutting performance. Construction and Building Materials, 224, 920–929. doi:10.1016/j.conbuildmat.2019.07.133.

[94] Faruk, A. N. M., Lee, S. I., Zhang, J., Naik, B., & Walubita, L. F. (2015). Measurement of HMA shear resistance potential in the lab: The simple punching shear test. Construction and Building Materials, 99, 62–72. doi:10.1016/j.conbuildmat.2015.09.006.

[95] Caputo, P., Porto, M., Angelico, R., Loise, V., Calandra, P., & Oliviero Rossi, C. (2020). Bitumen and asphalt concrete modified by nanometer-sized particles: Basic concepts, the state of the art and future perspectives of the nanoscale approach. Advances in Colloid and Interface Science, 285, 102283. doi:10.1016/j.cis.2020.102283.

[96] Hamedi, G. H., & Moghadas Nejad, F. (2015). Using energy parameters based on the surface free energy concept to evaluate the moisture susceptibility of hot mix asphalt. Road Materials and Pavement Design, 16(2), 239–255. doi:10.1080/14680629.2014.990049.

[97] Raufi, H., Topal, A., Sengoz, B., & Kaya, D. (2019). Assessment of Asphalt Binders and Hot Mix Asphalt Modified with Nanomaterials. Periodica Polytechnica Civil Engineering. doi:10.3311/ppci.14487.

[98] Kordi, Z., & Shafabakhsh, G. (2017). Evaluating mechanical properties of stone mastic asphalt modified with Nano Fe2O3. Construction and Building Materials, 134, 530–539. doi:10.1016/j.conbuildmat.2016.12.202.

[99] Seitllari, A., Boz, I., Habbouche, J., & Diefenderfer, S. D. (2023). Using mechanistic–empirical based analysis to evaluate rutting performance thresholds for balanced mix design tests. Construction and Building Materials, 400, 132762. doi:10.1016/j.conbuildmat.2023.132762.